Amplitude- and phase-resolved optical near fields of split-ring-resonator-based metamaterials

T. Zentgraf,[1,2,*] J. Dorfmüller,[2] C. Rockstuhl,[3] C. Etrich,[4] R. Vogelgesang,[2] K. Kern,[2] T. Pertsch,[4] F. Lederer,[3] and H. Giessen[1]

[1]*4. Physikalisches Institut, Universität Stuttgart, Pfaffenwaldring 57, 70550 Stuttgart, Germany*
[2]*Max-Planck-Institut für Festkörperforschung, Heisenbergstr. 1, 70569 Stuttgart, Germany*
[3]*Institute of Condensed Matter Theory and Solid State Optics, Friedrich Schiller University Jena, Max-Wien Platz 1, 07743 Jena, Germany*
[4]*Institute of Applied Physics, Friedrich Schiller University Jena, Max-Wien Platz 1, 07743 Jena, Germany*
**Corresponding author: t.zentgraf@fkf.mpg.de*

Received January 4, 2008; revised March 3, 2008; accepted March 9, 2008; posted March 17, 2008 (Doc. ID 91066); published April 14, 2008

We investigate the local optical response of split-ring resonator-(SRR)-based metamaterials with an apertureless scanning near-field optical microscope. By mapping the near fields of suitably resonant micrometer-sized SRRs in the near-infrared spectral region with an uncoated silicon tip, we obtain a spatial resolution of better than $\lambda/50$. The experimental results confirm numerical predictions of the near-field excitations of SRRs. Combining experimental near-field optical studies with near- and far-field optical simulations provides a detailed understanding of resonance mechanisms in subwavelength structures and will facilitate an efficient approach to improved designs. © 2008 Optical Society of America

OCIS codes: 160.3918, 160.4760, 310.6628, 160.3900.

In recent years much effort has been dedicated to exploring the properties of metamaterials. The ultimate goal is to control the effective material dispersion up to optical frequencies [1–3]. Along this avenue new designs were proposed, and the dimensions of critical feature sizes became smaller. The most prominent example for a metamaterial building block is the split-ring resonator (SRR) [4,5]. In general, SRRs consist of metallic structures much smaller than the light wavelength but much larger than the atomic scale. So far, resonance features of magnetic and dielectric properties in an effective medium that consists of periodically arranged SRRs were experimentally studied only in the far field [1,6,7]. It was found that a certain number of well-defined peaks occur in the reflection spectra for periodically arranged SRRs, where the peak at the lowest frequency (herein denoted as first-order eigenmode) can provide a dispersive response of the effective permeability in such a material [1]. Usually these investigations do not provide complete insight into the microscopic excitation mechanisms. Complementary near-field optical studies can therefore be of value to understand the character of such excitation mechanisms, leading to an improvement of the material response in new metamaterial designs.

In this Letter, we utilize an apertureless scanning near-field optical microscope (aSNOM) to detect the amplitude and phase of the near-field distributions of SRRs. All measurements are performed at a fixed wavelength to make the different results comparable. Therefore, we utilize the geometrical size effect of the SRRs to tune the resonances to the desired wavelength [7,8]. Such an approach provides the possibility to investigate different eigenmodes of the SRR at the same wavelength. All measurements are supported by numerical simulations, which are based on a finite-difference time-domain method.

The SRRs are fabricated by electron beam lithography and a subsequent dry etching technique on top of a 750 μm thick CaF_2 substrate. For the metal structures we used gold with a thickness of 60 nm. The fabricated patterns consist of two different sizes of SRRs, where the geometric sizes are approximately 500 nm $\times$ 500 nm for the small SRRs [denoted by superscript (S)] and 1.2 μm $\times$ 1.2 μm for the large SRRs [denoted by superscript (L)], respectively. Figures 1(a) and 1(b) show the obtained topographic information for the two different patterns. The geometric sizes of the SRRs appear slightly enlarged compared to the scanning electron microscopy images owing to the morphological convolution of the structure's shape with the probe tip shape, typical for atomic force microscopic imaging. Therefore, all structure sizes are obtained from these images [9].

Figure 1(c) shows the measured far-field reflectance spectra for two patterns of SRRs at a normal light incidence. The light polarization is set along the x direction. For the small SRRs the first- and third-order resonances (denoted by $1^{(S)}$ and $3^{(S)}$) [10] are clearly visible in the reflectance spectrum at 2.8 and 1.3 μm, respectively. In contrast, the large SRRs show the third-order resonance (denoted by $3^{(L)}$) at 3.0 μm, whereas the first-order resonance is shifted

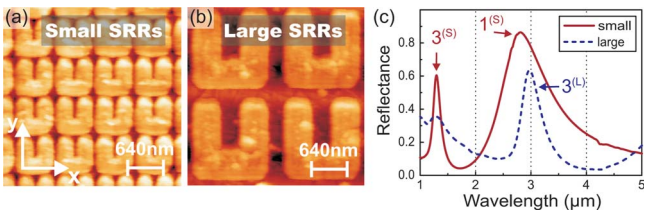

Fig. 1. (Color online) (a) and (b) Atomic force microscope topography images of the small/large structures. (c) Measured reflectance spectra for the two different SRR sizes.

to larger wavelengths outside the displayed spectral window.

For measurement of the amplitude and phase of the near fields of the SRRs, we utilized an aSNOM as described in [11]. The output of a cw optical parametric oscillator (Linos OS 4000) with a wavelength of 2.65 μm is used as the light source. This wavelength is slightly smaller than the resonance wavelengths of the structures. However, numerical calculations show that the near-field distribution only marginally changes for this off-resonance excitation. At the sample the excitation is s polarized along the x axis. The measurements are performed with an uncoated silicon tip that oscillates with an amplitude of 80 nm in noncontact mode above the sample, which is raster scanned underneath. With this technique we achieved information about the near fields with a spatial resolution of better than $\lambda/50$.

The incoming wave has an incidence angle of 73° with respect to the sample surface normal (z direction) owing to the excitation geometry in our setup. We measure the p-polarized component of the backscattered radiation. The signal is decomposed into time-harmonic Fourier components, because the position of the silicon tip in the z direction is harmonically modulated in time with a finite amplitude. Amplitude and phase of the second Fourier component are extracted, efficiently suppressing far-field background signals that contribute mostly to the zeroth order. Still, a slowly varying background is observed in the second order. Within one unit cell, however, it merely offsets the desired signal by a corresponding constant. The signs of the simulated signals are understood relative to this background.

Figure 2 shows the obtained near-field distributions (E_z component) for both structure sizes. The calculated near-field distributions are an exact reproduction of the experimental situation (described herein) with the only assumption that the silicon tip is neglected and not considered in the simulation. The periodic field distributions in Figs. 2(a) and 2(c) optically confirm the precise fabrication of the nanostructures. For the small SRRs the mode structure of the first-order eigenmode can easily be identified in the measured and calculated field distributions [a close-up for this mode is shown in Fig. 2(a) on the right side]. This fundamental mode is characterized by strong fields at the end of the two side arms of the SRR with a phase difference of π in between [12]. The physical origin of this behavior is an induced collective oscillation of the conduction band electrons of the metal along the SRR. This current gives a dipolelike response to the light field.

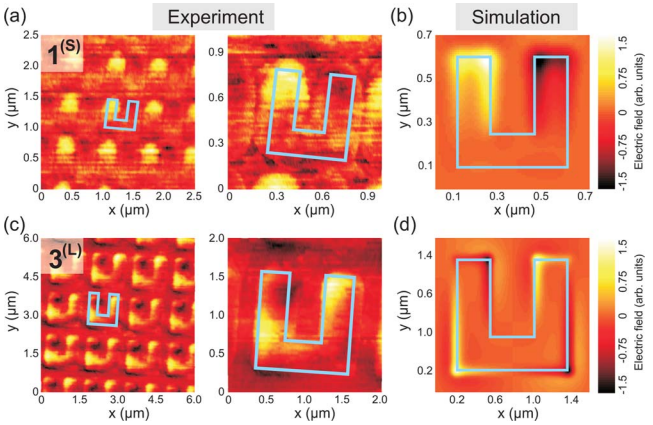

Fig. 2. (Color online) Measured and calculated electric field distributions (E_z component) of the first- and third-order eigenmodes for a wavelength of $\lambda = 2.65$ μm. (a) and (b) Results of the small SRRs with the dipolelike field; (c) and (d) results of the large SRRs with the quadrupolelike field for the third-order mode. The background color denotes the real part of the electric field component in the z direction. For better visibility, the one SRR is marked by the bold curve. The slight rotation is owing to sample misalignment.

Although the light incidence occurs at an angle of 73°, the near field is only marginally changed and appears nearly identical when compared with normal incidence (see Fig. 4 in [12]). This situation changes slightly for the near field of the third-order mode as shown in detail in Figs. 2(c) and 2(d). Nonetheless, the eigenmode structure with strong fields close to the four corners of the SRR is clearly visible both in the measurement and simulation. Note that the numerical simulations are accomplished for exactly the same excitation geometry as in the experiment. The field distribution of this higher-order mode shows a spatial profile comparable to an electric quadrupole field. Hence, it becomes clear that the quality factor of the third-order resonance of the large SRRs in Fig. 1(a) is three times larger than that of the fundamental (dipolelike) mode in the small SRRs. This fact is owing to the lower radiation losses by the weaker coupling of the quadrupole field to the linearly polarized excitation.

Although the measured and simulated results qualitatively agree, some deviations can occur owing to the influence of the silicon probing tip that were not taken into account in the simulations. However, the deviations between the measurements and simulations are small. Therefore, we conclude that the impact of the silicon tip is only of minor significance for the experimental results shown. This is in contrast to near-field measurements with metal-coated probes that can strongly influence the local fields of nanostructures and change their resonance behavior [13].

Furthermore, the comparison between the measured and calculated fields unambiguously shows that the tip mainly detects the z component (the component perpendicular to the surface) of the electric field. The x and y components of the electric field are strongly suppressed and do not contribute to the measurable signal.

Finally, we compare the first-order eigenmode of the SRR to the fundamental eigenmode of a cut wire, which can also be regarded as an unfolded SRR [8]. As the spectral resonance behavior of both structures has the same origin (plasmonic eigenmode excitation of the conduction band electrons), the near fields should show an analogous characteristic. For this measurement, another sample was fabricated with an array of single cut-wire pieces. The wires have a size of 1000 nm $\times$ 300 nm and the same height as the

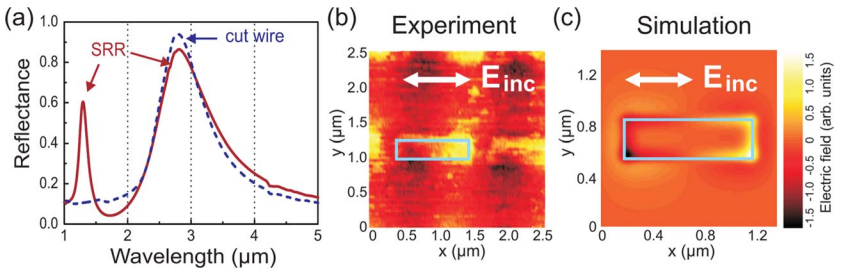

Fig. 3. (Color online) (a) Measured reflectance spectrum for the small SRRs in comparison with the measured spectrum for the cut-wire pieces (unfolded SRR). Both structures have nearly the same entire length and show a strong peak in the reflectance at the same spectral position. (b) Measured and (c) calculated electric field distributions of the cut wire for $\lambda = 2.65\ \mu$m. E_{inc} denotes the electric field polarization of the incident wave. For better visibility, the cut wire is marked by a bold curve.

SRRs. For this selected size, the resonance wavelength of the cut wires matches the first-order eigenmode of the small SRRs. Figure 3(a) shows the spectral response of the reflectance of the cut-wire pieces in comparison with the small SRRs. The far-field spectra show exactly the same spectral response for both structures with a single exception; the third-order mode, which is clearly visible at 1.3 μm for the SRRs, is not excited for the cut wires. The symmetry of the wire structure strongly reduces the excitation efficiency of this mode.

The measured and simulated near fields of the cut wires are shown in Figs. 3(b) and 3(c), respectively. Again, the numerical calculation in Fig. 3(c) shows good qualitative agreement with the measurement. The near field exhibits strong electric fields at both ends of the wire with a phase jump of π in between. This is the typical field distribution of an electric dipole excitation (i.e., dipole antenna). Note that the calculation displays only the z component of the electric field (the second Fourier component of the time-harmonic tip oscillation). Hence, the field distribution exactly resembles the field of the first-order eigenmode of an unfolded SRR that shows the same strong field components in the z direction at both ends of the ring structure. The measurement confirms the assumption of [8,12] that the resonances in SRRs are owing to the excitation of localized surface plasmon polaritons in the ring structure. The measurement of the near field is in some sense a complementary far-field spectroscopy; it allows the direct observation of the underlying processes of spectral features in the far field without utilizing a complex numerical simulation.

In conclusion, we experimentally investigated the near-field distribution of SRR metamaterials with an aSNOM in the near-infrared spectral region. Different sizes of SRRs are used to tune the resonance wavelength of the different eigenmodes to the same spectral position. The measurements of the optical near field of such structures confirm the model of plasmonic excitations for the different spectral features in the far-field spectrum. Numerical simulations support the measurements and show that the electric field component perpendicular to the surface is detected mainly with such an aSNOM technique. The measurements will help to obtain a detailed understanding of the underlying excitation processes of resonances in such metamaterials and can facilitate the search for efficient approaches to improved designs. Near-field measurements open up the possibility of designing and utilizing local structure variations with the final goal of functional devices in the field of metamaterials.

This work was supported by the Federal Ministry of Education and Research (grant 13N9155) and the Deutsche Forschungsgemeinschaft (grants FOR557 and FOR730). T. Zentgraf acknowledges support from the Landesstiftung Baden-Württemberg.

References and Notes

1. S. Linden, C. Enkrich, M. Wegener, J. Zhou, T. Koschny, and C. M. Soukoulis, Science **306**, 1351 (2004).
2. V. M. Shalaev, W. Cai, U. K. Chettiar, H.-K. Yuan, A. K. Sarychev, V. P. Drachev, and A. V. Kildishev, Opt. Lett. **30**, 3356 (2005).
3. S. Zhang, W. Fan, N. C. Panoiu, K. J. Malloy, R. M. Osgood, and S. R. J. Brueck, Phys. Rev. Lett. **95**, 137404 (2005).
4. J. P. Pendry, A. J. Holden, D. J. Robbins, and W. J. Stewart, IEEE Trans. Microwave Theory Tech. **47**, 2075 (1999).
5. T. J. Yen, W. J. Padilla, N. Fang, D. C. Vier, D. R. Smith, J. B. Pendry, D. N. Basov, and X. Zhang, Science **303**, 1494 (2004).
6. N. P. Johnson, A. Z. Khokhar, H. M. Chong, R. M. De La Rue, T. J. Antosiewicz, and S. McMeekin, Opto-Electron. Rev. **14**, 187 (2006).
7. C. Rockstuhl, T. Zentgraf, H. Guo, N. Liu, C. Etrich, I. Loa, K. Syassen, J. Kuhl, F. Lederer, and H. Giessen, Appl. Phys. B **84**, 219 (2006).
8. H. Guo, N. Liu, L. Fu, H. Schweizer, S. Kaiser, and H. Giessen, Phys. Status Solidi B **244**, 1256 (2007).
9. Additional parameters for the small structures (large structures) are the linewidth of 150 nm (360 nm) and the period of 0.7 μm (1.62 μm), which is identical in the x- and y-directions.
10. The number directly indicates the number of nodal lines in the planar field pattern cut of the z component of the electric field and is consistent with the denotation in [12].
11. A. Bek, R. Vogelgesang, and K. Kern, Rev. Sci. Instrum. **77**, 043703 (2006).
12. C. Rockstuhl, F. Lederer, C. Etrich, T. Zentgraf, J. Kuhl, and H. Giessen, Opt. Express **14**, 8827 (2006).
13. M. Abashin, U. Levy, K. Ikeda, and Y. Fainman, Opt. Lett. **32**, 2602 (2007).